Semipolar AlGaN layers on a nano-structured Si(100) substrate

© V.N. Bessolov[1], A.Yu. Ivanov[2], M.E. Kompan[1], E.V. Konenkova[1],
A.V. Solomnikova[3], Sh.Sh. Sharofidinov[1]

[1] Ioffe Institute,
St. Petersburg, Russia
[2] ITMO University,
St. Petersburg, Russia
[3] St. Petersburg State Electrotechnical University „LETI",
St. Petersburg, Russia
E-mail: lena@triat.ioffe.ru

Received February 19, 2026
Revised March 6, 2026
Accepted March 12, 2026

Structural and spectroscopic diagnostic methods were used to study AlGaN layers grown by the method of hydride vapour-phase epitaxy on a Si(100) substrate with a V-shaped nanostructure on the surface (NP-Si(100) substrate) and an AlN buffer layer deposited by the reactive magnetron sputtering method. X-ray diffraction analysis showed that the use of a low-temperature AlN buffer layer provides a tendency for AlN blocks to crystallize with a non-polar $(10\bar{1}0)$ orientation. The NP-Si(100) substrate, with a thickness of $10\,\mu$m, forms a block configuration of the $Al_xGa_{1-x}N$ layer associated with semi-polar orientations $(10\bar{1}3)$ and $(10\bar{1}5)$ with $x = 0.42$ and $x = 0.39$, respectively. The layer diffraction pattern shows the presence of blocks with a polar hexagonal $Al_xGa_{1-x}N$ with $x = 0.36$, and cubic c-AlN(220) and c-AlN(420) crystallographic orientations. The atomic force microscopy showed that the $150\,\mu$m thick AlGaN layer has block sizes of $9\,\mu$m and a semi-polar crystal orientation. The layer diffraction pattern shows the presence of blocks with a polar hexagonal $Al_xGa_{1-x}N$ with $x = 0.36$, and cubic c-AlN(220) and c-AlN(420) crystallographic orientations. The AFM showed that the $150\,\mu$m thick AlGaN layer has block sizes of $9\,\mu$m and a semipolar crystal orientation.

Keywords: semipolar AlGaN, nano-structured silicon substrate Si(100), hydride vapour-phase epitaxy.

DOI: 10.61011/SC.2026.01.63728.9123

1. Introduction

In recent years, huge strides have been made in the field of III-nitride-based optoelectronics on sapphire substrates, related to both, polar GaN grown emitters and devices combining lighting and communication functions and capable of providing very high data transmission rates. One of the main problems that stems the rise of efficiency of emitting structures is the polar orientation of c-plane of GaN, which leads to the emergence of piezoelectric fields in devices with InGaN/GaN quantum wells because of mismatch of InGaN and GaN lattices. Emitters based on polar III-nitride layers exhibit less overlap of the wave functions of electrons and holes, resulting in a longer radiative recombination period and, consequently, a decline in quantum efficiency, the so-called quantum-limited Stark effect.

One promising approach to increasing the efficiency of electronic devices is to grow heterostructures in a semi-polar or non-polar direction, which can reduce or eliminate internal electric fields.

However, deviation of the structures from the polar orientation results in emergence of additional defects and mismatch dislocations, in addition to dislocations that are present in heteroepitaxial III-nitride layers with c-orientation. Epitaxial growth of semipolar $Al_xGa_{1-x}N$ layers is associated with additional challenges that can significantly impact the performance of semipolar devices. When using hydride vapor-phase epitaxy (HVPE) method, AlN grows from $AlCl_3$ under practically nonequilibrium conditions, and GaN grows from GaCl under conditions close to equilibrium. Obtaining uniform AlGaN layers presents a certain difficulty, since the rates of formation of AlN and GaN nuclei differ significantly, and the mean free path of an Al atom on the AlN surface is 40 nm, while that of a Ga atom on the GaN surface is 500 nm [1]. As a rule, known models predict the sensitivity of AlGaN composition to changes in flow rates and to the ratio III/V [2].

Thermodynamic analysis of HVPE AlGaN using $AlCl_3$ and GaCl is outlined in [3], where the authors showed that controlled layer growth is possible under certain epitaxy parameters. Epitaxial growth of AlGaN layers by HVPE method on both GaN and AlN templates on a sapphire substrate showed good structural quality of the obtained layers [4]. Semi-polar AlGaN$(11\bar{2}2)$ was grown on a sapphire substrate with m-plane, but its quality was low [5]. Recently, all high-index orientations of Si have been theoretically predicted, which allow the growth of AlN layers with semi-polar orientation [6].

Previously, we demonstrated HVPE method for epitaxy of thick semi-polar AlN$(10\bar{1}1)$ layers on a nanostructured Si(100) [7] substrate. This paper continues research in this field and covers the features of the growth of semi-polar AlGaN layers on a nano-structured silicon substrate.

2. Experiment procedure

First, a series of stripes located on the surface of Si(100) substrate were formed using interference lithography. Then, using anisotropic etching with potassium hydroxide, V-shaped NP-Si(100) grooves were formed, consisting of Si($\bar{1}$11) and Si(1$\bar{1}$1) surfaces adjacent at an angle of 54.7°, similar to [7].

NP-Si(100) substrates had grooves with an average period of $\sim$ 60 nm, a height of $\sim$ 50 nm and underwent a standard procedure of cleaning and etching in an aqueous solution of hydrofluoric acid. Initially, for one type of structures, a 100 nm thick AlN buffer layer was grown using magnetron sputtering in a plasma mixture N_2/Ar at $T = 450\,^\circ$C, while the other type did not have a buffer layer. Epitaxial growth of AlGaN layers was carried out by HVPE method in argon atmosphere at temperatures 1050–1080 °C, with a thickness of 10 to 150 μm with a growth rate $\sim 1\,\mu$m/min similar to [7]. Two types of structures „A" — with a buffer layer of AlN, „B" — without any buffer layer. The crystalline properties of AlN layers were estimated using X-ray diffractometry, atomic force microscopy (AFM) and Raman scattering (RS). The studies were carried out using an X-ray diffractometer DRON-8. RS was made using Raman spectrometer JY HORIBS MRS 320. The light source was a helium-neon laser with a wavelength of 632.8 nm. AFM measurements were carried out in the tapping mode using a scanning probe microscope Solver NEXT.

3. Results and discussion

The formation of AlN buffer layer showed that it is deposited in the direction perpendicular to Si(111) and Si(1$\bar{1}\bar{1}$) planes (Figure 1).

In the lower part of the groove, one can observe formation of layers on both faces, and the thickness of the layer on Si(111) — h_1 face is greater than that of the layer on Si(1$\bar{1}\bar{1}$) — h_2 face (Figure 1), which indicates the preferential growth of layers in one of the directions. As a rule, AlN buffer layers obtained at low temperatures by magnetron sputtering are polycrystalline in nature. Some of the surface planes of AlN blocks have inclinations of up to 58°, which differs from the inclination of Si(111) — 54.7° relative to Si(100) plane (Figure 1). This will likely lead to the formation of semi-polar blocks with different crystal orientations in „A" sample. In „B" sample the heterogeneity of the blocks is explained by different inclination of the edges along the groove.

The X-ray diffraction analysis of „A" and „B" structures showed (Figure 2, a, b), that the layers had a complex block layer configuration associated with semipolar planes $Al_xGa_{1-x}N$ (10$\bar{1}$3) and (10$\bar{1}$5) with $x = 0.42$ and $x = 0.39$

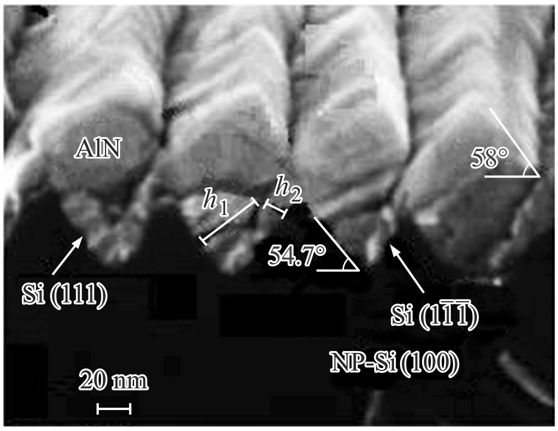

Figure 1. SEM (scanning electron microscopy) image of AlN buffer layer on NP-Si(100) substrate.

Reflectance peaks, composition and structure of the block layer

2θ, deg.	Reflection	Material
33.10	10$\bar{1}$0	h-AlN
35.09	0002	h-AlGaN, $x = 0.36$
61.71	220	c-AlN
64.49	10$\bar{1}$3	h-AlGaN, $x = 0.42$
69.16	400	c-Si
107.14	10$\bar{1}$5	h-AlGaN, $x = 0.39$
116.62	420	c-AlN

respectively, with polar $Al_xGa_{1-x}N$ with $x = 0.36$ and cubic c-AlN(220) and c-AlN(420) crystallographic blocks (see the Table below). In „A" sample the peaks associated with a non-polar hexagonal AlN(10$\bar{1}$0) were observed.

In the Raman spectra of $Al_xGa_{1-x}N$/AlN/NP-Si(100) structure, the peaks E_2(high) $= 652.6\,\mathrm{cm}^{-1}$, associated with AlN, and E_2(high) $= 575.9\,\mathrm{cm}^{-1}$, which, similar to [8], can be attributed to $Al_{0.3}Ga_{0.7}N$ (Figure 3) were observed.

As is known, the peak E_2(high) for unstressed AlN is located around $657.0\,\mathrm{cm}^{-1}$ [9]. It can be seen that the position of the peak of E_2(high) line for AlN blocks is shifted to the low-frequency side relative to its position in the undeformed layer, which indicates a tensile strain acting in AlGaN/NP-Si(100) structure. AFM image of a 150 μm thick structure's surface demonstrates that AlGaN has a block character with a block size of $\sim 9\,\mu$m (Figure 4, a), and the surface profile indicates the semi-polar character of the layer (Figure 4, b).

It is known that during AlN epitaxy, layers are formed at different rates on the edges of AlN/Si(111) and AlN/Si(1$\bar{1}\bar{1}$) grooves, and the highest growth rate leads to the formation of a semi-polar layer in one of two possible directions, namely AlN(10$\bar{1}$1) [7]. It's a well-known fact that AlGaN nucleus faces usually originate complying with Gibbs-Curie-Wulff principles [10]. The nucleation of AlGaN crystals with different crystalline orientations is associated with the characteristics of „A" and „B" samples and a sufficiently

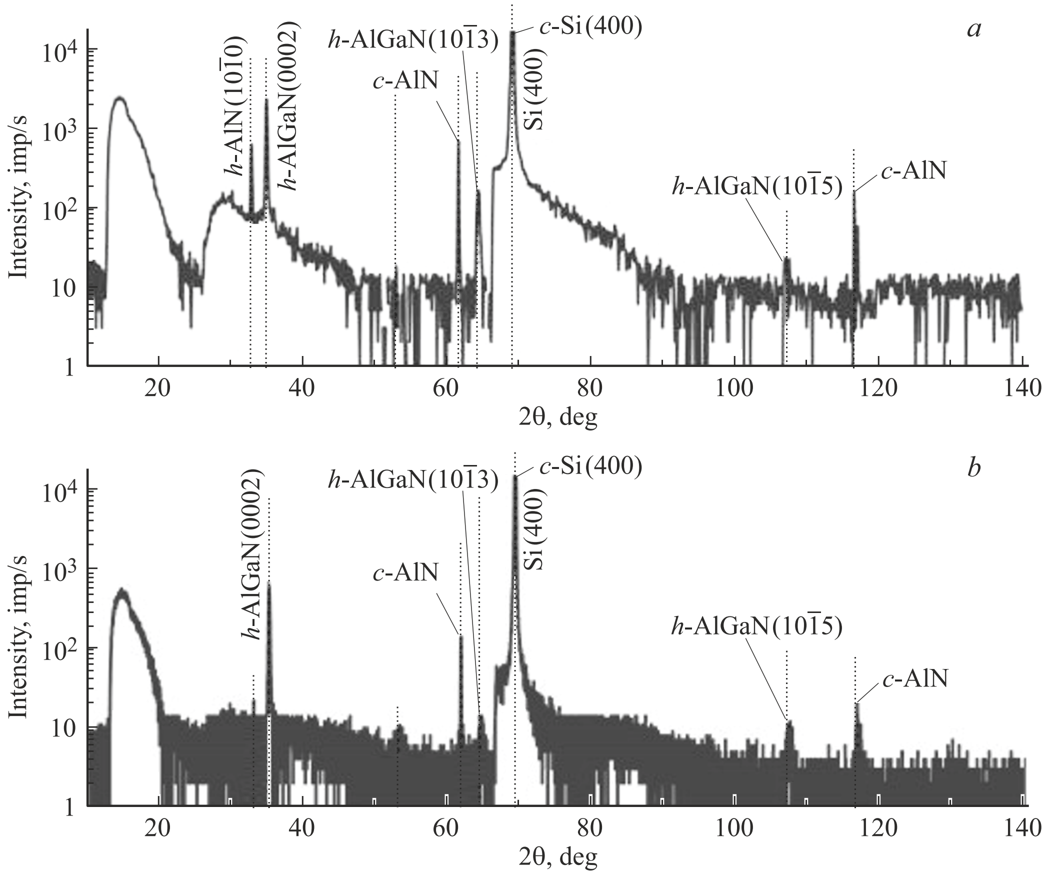

Figure 2. Diffraction pattern of AlGaN for two types of structure NP-Si(100): *a* — „A“, *b* — „B“.

high growth rate in HVPE method. The formation of *c*-AlN crystals in „A“ sample is either associated with the formation of a microcrystalline block layer at low temperatures by magnetron sputtering, which also includes nanocrystals of cubic AlN [11], which form blocks during further growth of the layer, or the emergence of *c*-AlN crystals in the samples is possibly associated with the transition of the layer hexagonal modification into a cubic one during epitaxy in *V*-shaped groove, when two growth fronts meet [12].

The formation of *c*-AlN(022), AlN(004) crystals during epitaxy on Si(100) substrates was observed in the study [13] and is associated with the crystallographic ratio AlN(100)/Si(100). In our case, when AlN is generated in „B“ sample the bottom of the groove may have Si(100) sections.

The formation of semi-polar crystals AlGaN(10$\bar{1}$3) and AlGaN(10$\bar{1}$5) is apparently associated with specifics of the blocks formation on Si(111) and Si(1$\bar{1}\bar{1}$) faces (sample „B“), while, apparently, for „A“ sample the buffer layer with a thickness of 100 nm is not an obstacle to the formation of a semi-polar layer. The formation of blocks with non-polar orientation AlN(10$\bar{1}$0) only in „A“ sample is likely because of the effect discovered in [14]. During HVPE epitaxy in an argon atmosphere, a spontaneous change in

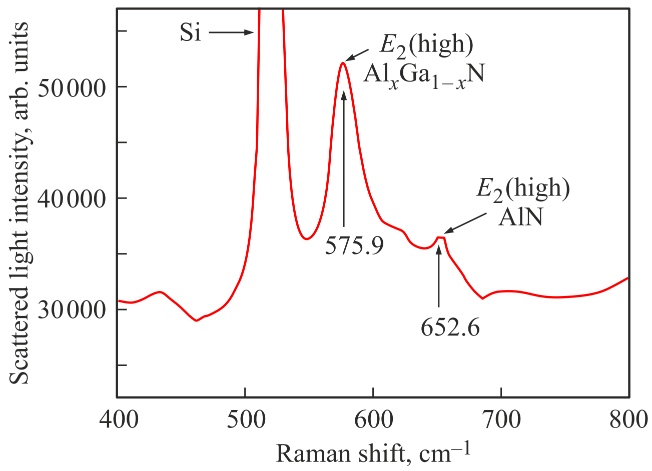

Figure 3. RS spectra of AlGaN/AlN/NP-Si(100).

growth orientation from polar to non-polar is possible during growth on *c*-plane of a sapphire substrate. In „A“ sample, in contrast to „B“ the layer growth by HVPE method occurs on a microcrystalline AlN layer, the surface of which oxidizes when moving from the magnetron sputtering reactor. Al oxides can have microcrystals with faces with

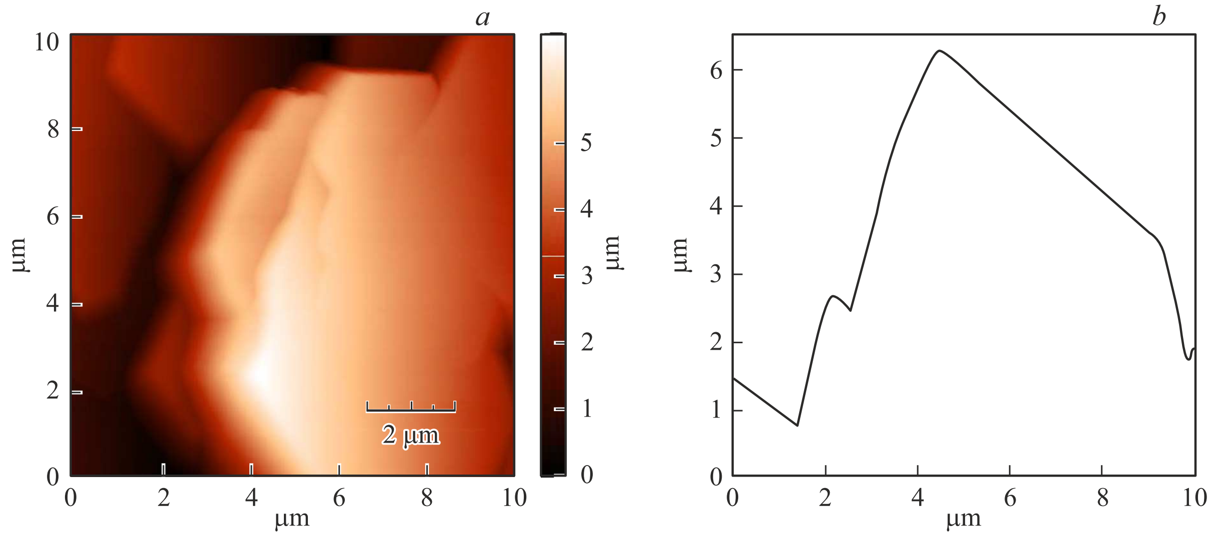

Figure 4. Topography (a) and surface profiles in the direction perpendicular to the „nanogroove" (b) of AlGaN/NP-Si(100) structure.

r-oriented planes. With this model, with further high-rate growth of the layer by HVPE method in an argon atmosphere, a non-polar layer may emerge [14].

As the layer grows, competition between blocks in the layer can partially explain the formation of layers of predominantly one phase. According to the model, if the formation energy of one phase is less than that of another, and the barrier is lower, then in this case, this phase will most likely dominate in the process of block layer growth [15]. As the growth proceeds, the block sizes increase, which is reflected in the AFM image (Figure 4, a).

4. Conclusion

AlGaN layers grown by method of hydride vapor-phase epitaxy (HVPE) on a Si(100) substrate, on the surface of which a symmetric V--shaped nanostructure and AlN buffer layer obtained by reactive magnetron sputtering were formed, were studied. X-ray diffraction analysis showed that the use of a low-temperature AlN buffer layer ensures the tendency of AlN blocks with non-polar $(10\bar{1}0)$ orientations to crystallize. The NP-Si(100) substrate with a thickness of $10\,\mu$m forms a block configuration of the $Al_xGa_{1-x}N$ layer associated with semi-polar orientations $(10\bar{1}3)$ and $(10\bar{1}5)$ with $x = 0.42$ and $x = 0.39$, respectively. Blocks with polar hexagonal $Al_xGa_{1-x}N$ with $x = 0.36$ and cubic c-AlN(220) and c-AlN(420) crystallographic orientations were found in the layer. In the Raman spectra of $Al_xGa_{1-x}N$/AlN/NP-Si(100) structure, the peak $E_2(\text{high}) = 652.6\,\text{cm}^{-1}$ associated with AlN and the peak $E_2(\text{high}) = 575.9\,\text{cm}^{-1}$, which can be attributed to $Al_{0.3}Ga_{0.7}N$, emerged. AFM showed that the $150\,\mu$m thick AlGaN layer has block sizes of $9\,\mu$m and a crystalline semi-polar (10=13) orientation. The results of this study provide a foundation for the technology of semi-polar AlGaN/Si heterostructures, paving the way for innovative applications in optoelectronics.

Acknowledgments

The authors wish to thank the Scanning Microscopy Center of St. Petersburg Electrotechnical University „LETI" and OOO Aktivnaya Fotonika for performing the AFM measurements.

Conflict of interest

The authors declare that they have no conflict of interest.

References

[1] M. Sobanska, Z.R. Zytkiewicz, K. Klosek, R. Kruszka, K. Golaszewska, M. Ekielski, S. Gieraltowska. Nanotechnology, **31**, 184001 (2020).
https://doi.org/10.1088/1361-6528/ab6bf2

[2] A.S. Segal, D.S. Bazarevskiy, M.V. Bogdanov, E.V. Yakovlev. Phys. Status Solidi C, **6** (S2), S329 (2009).
https://doi.org/10.1002/pssc.200880892

[3] A. Koukitu, J. Kikuchi, Y. Kangawa, Y. Kumagai. J. Cryst. Growth, **281** (1), 47 (2005).
https://doi.org/10.1016/j.jcrysgro.2005.03.010

[4] H. Fujikura, T. Konno, T. Kimura. Appl. Phys. Express, **15**, 085504 (2022). https://doi.org/10.35848/1882-0786/ac8412

[5] Q. Chen, J. Dai, X. Li, Y. Gao, H. Long, Z.-H. Zhang, Ch. Chen, H.-Ch. Kuo. IEEE Electron Dev. Lett., **40** (12), 1925 (2019). https://doi.org/10.1109/LED.2019.2948952

[6] J.-L. Li, Y.-F. Li, Zh.-P. Liu. Nature Commun., **16**, 4303 (2025). https://doi.org/10.1038/s41467-025-59613-5

[7] V.N. Bessolov, M.E. Kompan, E.V. Konenkova, Sh.Sh. Sharofidinov, A.V. Solomnikova, M.P. Shcheglov. Pis'ma ZhTF **4**, 25 (2026) (in Russian).
https://doi.org/10.61011/PJTF.2026.04.62321.20500

[8] M. Kuball. Surf. Interface Anal., **31**, 987 (2001). https://doi.org/10.1002/sia.1134

[9] W. Zheng, R. Zheng, F. Huang, H. Wu, F. Li. Photon. Res., **3** (2), 38 (2015). https://doi.org/10.1364/prj.3.000038

[10] *Sovremennaya kristallografiya*. V. 3. *Obrazovaniye kristallov*, ed. by B.K. Weinstein, A.A. Chernov, L.A. Shuvalov (M., Nauka, 1980).

[11] A. Pandey, R. Prakash, Sh. Dutta, S. Dalal, A. Kumar, A.K. Kapoor, D. Kaur. AIP Conf. Proc., **1953**, 100028 (2018). https://doi.org/10.1063/1.5032964

[12] D.M. Waters, B. Thompson, G. Ferenczi, B. Hourahine, G. Cios, A. Winkelmann, Ch.J.M. Stark, Ch. Wetzel, C. Trager-Cowan, J. Bruckbauer. J. Appl. Phys., **137**, 045701 (2025). https://doi.org/10.1063/5.0244438

[13] W.-T. Lin, L.-Ch. Meng, G.-J. Chen, H.-Sh. Liu. Appl. Phys. Lett., **66**, 2066 (1995). https://doi.org/10.1063/1.113904

[14] V. Ivantsov. Cryst. Growth Des., **23** (5), 3805 (2023). https://doi.org/10.1021/acs.cgd.3c00180/

[15] L. Zhang, J. Wu, T. Han, F. Liu, M. Li, X. Zhu, Q. Zhao, T. Yu. Cryst. Eng. Commun., **23**, 3364 (2021). https://doi.org/10.1039/D1CE00040C

Translated by T.Zorina